Received: 18 June 2018 | Revised: 6 November 2018 | Accepted: 2 December 2018

DOI: 10.1002/acm2.12525

RADIATION ONCOLOGY PHYSICS

WILEY

Optimization of skin dose using *in-vivo* MOSFET dose measurements in bolus/non-bolus fraction ratio: A VMAT and a 3DCRT study

Anabela G. Dias[1,2] | Diana F. S. Pinto[3] | Maria F. Borges[1] | Maria H. Pereira[3] | João A. M. Santos[1,2,4] | Luís T. Cunha[1,2] | Joana Lencart[1,2]

[1]Medical Physics Department, Portuguese Institute of Oncology (IPO-Porto), Porto, Portugal

[2]Medical Physics, Radiobiology and Radiation Protection Group, Research Centre, Portuguese Institute of Oncology, Porto (CI-IPO), Portugal

[3]Radiotherapy Department, Portuguese Institute of Oncology, Porto, Portugal

[4]Abel Salazar Institute of Biomedical Sciences (ICBAS), University of Porto, Porto, Portugal

Author to whom correspondence should be addressed: Anabela G. Dias
E-mail: adias4@gmail.com

Abstract

In-phantom and *in-vivo* three dimensional conformal radiation therapy (3DCRT) and volumetric modulated arc therapy (VMAT) skin doses, measured with and without bolus in a female anthropomorphic phantom RANDO and in patients, were compared against treatment planning system calculated values. A thorough characterization of the metal oxide semiconductor field effect transistor measurement system was performed prior to the measurements in phantoms and patients. Patients with clinical indication for postoperative external radiotherapy were selected. Skin dose showed higher values with 3DCRT technique compared with VMAT. The increase in skin dose due to the use of bolus was quantified. It was observed that, in the case of VMAT, the bolus effect on the skin dose was considerable when compared with 3DCRT. From the point of view of treatment time, bolus cost, and positioning reproducibility, the use of bolus in these situations can be optimized.

PACS
87.53.Dq, 87.55.D-

KEY WORDS
bolus, breast carcinoma, *in-vivo* dosimetry, MOSFETs, skin dose

1 | INTRODUCTION

Skin injury is a known consequence of breast external radiotherapy treatments. These effects occur particularly in areas subjected to friction such as axilla and skin folds.[1,2] The severity of these radiation-induced side effects depends on several factors such as radiotherapy treatment modality and planning details; for instance fractionation, total dose, use of bolus, field modifiers, site, concurrent chemotherapy, and the use of biological agents.[1–7] Skin reactions become more evident toward the end of the treatment with their highest severity generally occurring in the first 2 weeks after the end of the treatment.[1–4,8]

The skin is generally considered an organ at risk and the minimization of the skin dose is a concern after breast conservative and mastectomy postoperative irradiation. However, in some cases, as inflammatory breast cancer or locally advanced breast cancer T4, the delivery of therapeutic dose to the skin is clinically beneficial. In this situation it is necessary to calculate and measure the superficial dose.[3,4,10–12] The precision of skin dose assessment is essential to guarantee that on one hand, the dose is below the tolerance levels

and, on the other hand, required doses should be high enough to avoid tumor recurrence.[3,4,6,10–12] Dose prescription and dosimetry assessment in the skin is not a straightforward task due to the limitation of treatment planning system (TPS) when calculating dose at the surface and at different structures of the skin (basal and dermal layers), as depth and location vary between patients and even in the same patient. The majority of available dose calculation algorithms are not sufficiently accurate to compute dose distributions in superficial and build-up regions where electron equilibrium is not established. Generally, TPS can calculate skin dose (build-up region) with accuracy up to 20%.[11–15]

Different methodologies for skin dose measurement and detectors characterization have been reported in the literature: radiochromic films; thermoluminescent dosimeters (TLD), and other passive solid state dosimeters; diodes; metal oxide semiconductor field effect transistors (MOSFETs)-based dosimeter, etc.[7,13,16–36]

The purpose of this work is to assess the skin doses in breast cancer treatments obtained with volumetric modulated arc therapy (VMAT) and three dimensional conformal radiation therapy (3DCRT) treatment techniques, using *in-vivo* dosimetry, and compare the measured values with the doses calculated by the TPS.

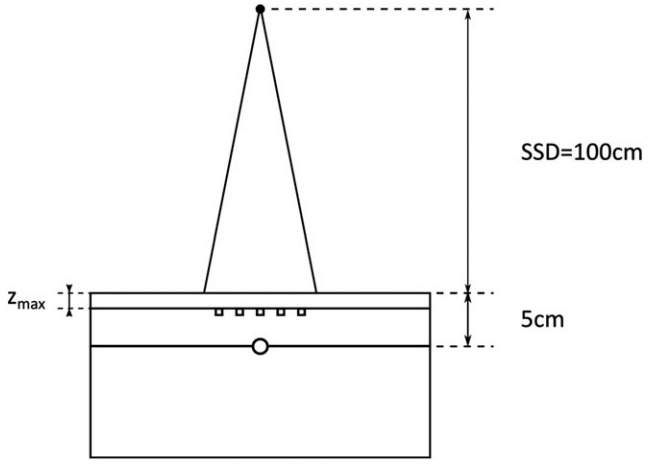

FIG. 1. System calibration setup. The ionization chamber positioned at a depth of 5 cm and the MOSFET detectors at Z_{max} depth for the specific energy.

2 | MATERIALS AND METHODS

2.A | MOSFET calibration

In this study, dual-bias TN502RD MOSFET detectors fabricated by Thomson & Nielsen, Canada, were used. Before performing the skin dose measurements, the MOSFET detectors were calibrated using 4 and 6 MV photon beams using a Varian 2100C/D and a 2300IX linac (Varian Medical Systems, Palo Alto, USA), respectively. The detectors were calibrated using a PMMA MOSFET calibration jig (Arplay Medical Products #TN-RD-57-30) in a solid water phantom (RW3 produced by PTW Freiburg GmbH, Freiburg, Germany) with source to surface distance (SSD) of 100 cm and a field size of 10 cm × 10 cm. A set of three detectors was placed in the central groves of the jig, with the flat side facing the beam, being the reference point at the position of the maximum dose (Z_{max}) of each energy. A 0.6 cm^3 Farmer ionization chamber (PTW 30013 PTW, Freiburg — Germany) was positioned at a depth of 5 cm for dose calibration verification (Fig. 1). The dose was calculated according to IAEA Technical Report Series (TRS) 398 protocol.[37] The presence of the MOSFET did not disturb the ion-chamber measurement as verified by our measurements. The MOSFET software (mobile MOSFET, Best® medical Canada) enables the determination of the calibration factor (CF) by averaging three consecutive measurements which are user validated.

2.B | MOSFET measurement system characterization methodology

A thorough characterization of the MOSFET-based dosimetry system was performed regarding linearity, reproducibility, and angular dependence for two photon energies commonly used in radiotherapy treatments of the breast (4 and 6 MV). All measurements, with the exception of the angular dependence, were performed using the standard setup above described for the calibration. The angular dependence was performed using a spherical phantom of 14 cm in diameter (Lucy 3D QA phantom – Standard Imaging, Middleton, USA) acquiring measurements with several beam incidences (45 degree increments; Fig. 2).

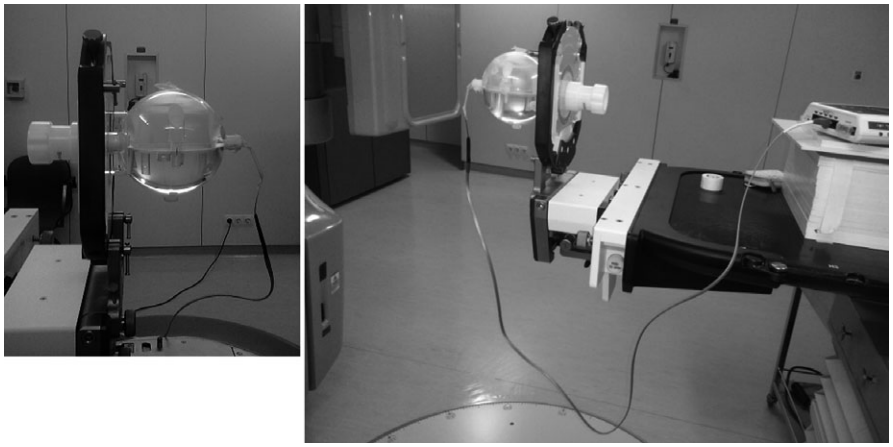

FIG. 2. Angular dependence measurement setup, with Lucy 3D quality assurance phantom.

To assess the variation of the dosimeters response with dose, three MOSFET located at the build-up position of each energy were irradiated in the range of 10 to 350 cGy with SSD = 100 cm. As a control measure (cross calibration), in the same procedure dose measurements were performed using the ionization chamber positioned at a 5 cm depth.

To assess the angular dependence, a MOSFET was placed in the center of the spherical phantom at the isocenter and a series of measurements was carried out by varying the rotation angle of the gantry. The MOSFET was positioned so that its flat side was facing the beam, with the gantry in the 0° position. The gantry angle varied between 0 and 315° in 45° increments.

2.C | In-phantom measurements methodology

The *in-phantom* measurements were performed using an anthropomorphic female RANDO phantom without breasts to simulate a post-mastectomy patient. A CT scan of the phantom was acquired and four measurement points were selected on the phantom surface as seen in Fig. 3: two corresponding to the entrance and the exit of tangent beams and two over the planning target volume (PTV), corresponding to points 2 cm from each side of the usual location of the surgical scar.

The clinical importance of measuring dose in this area is due to the relative high probability of future relapse.[6–9] The fourth point (P_4) was referenced on the axillar area, corresponding to the beam axis projection in the surface. The maximum sensitivity points of the MOSFET detectors were accurately placed on points P_1–P_4 and measurements were performed with and without bolus.

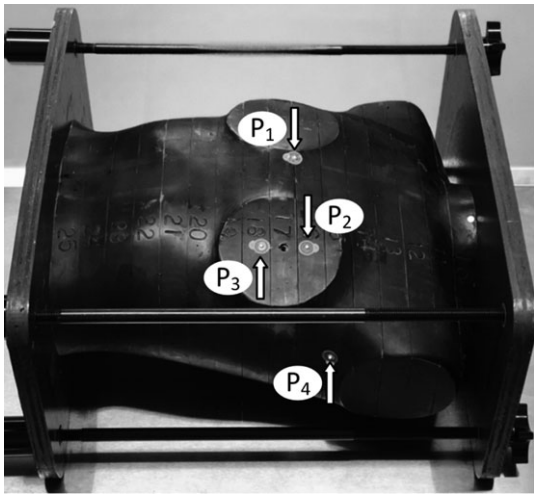

FIG. 3. Position of the four measurement points on the female RANDO chest wall.

The output from the TPS calculation on these points was later compared with the MOSFET measured doses. For this purpose, we used the TPS version 13.5 Eclipse® Varian (Varian Medical Systems, Inc., Palo Alto, CA, USA) using the Anisotropic Analytical Algorithm (AAA) with a calculation grid of 2.5 mm. 3DCRT treatment plans were performed in the RANDO phantom for the breast area, using two oblique opposing tangential fields in field-in field technique with 4 MV photon beams. The VMAT plans were performed with 6 MV using two partial arcs, in the right side from 60° to 181° and in the left side from 340° to 179°.

A 3DCRT and a VMAT plan similar to a clinical case using 4 and 6 MV, respectively, was performed, with and without a bolus (Super-Flab, Eckert & Ziegler, 1 cm thick) for surface dose enhancement. The prescription was 2 Gy (average dose in the PTV) per fraction for a total dose of 50 Gy in 25 fractions. In the TPS, the bolus was added, based on previous acquires CT unit calibration and no extra CT was performed to the patient.

2.D | *In-vivo* measurements methodology

After characterization and dose measurements on the skin of the anthropomorphic phantom, *in-vivo* measurements were performed in 20 patients with breast carcinoma undergoing treatment with two different irradiation techniques: 3DCRT and VMAT. For patients with high-risk for skin involvement or inflammatory cancer, the hospital protocol recommends the use of bolus in the last 10 fractions for skin dose enhancement. From the total number of selected patients, fourteen underwent treatment with VMAT technique and six with 3DCRT technique.

The CT scan was acquired with 2.5 mm slice spacing, extended from below the level of the orbits, when treatment includes regional lymph node irradiation or from the mandible, in the other cases, to about 5 cm below the ipsilateral or contralateral inframammary sulcus, in the case of mastectomized patients. During patient simulation, in addition to the positioning tattoos, four points corresponding to the measurement positions previously described (Section 2.C) were also tattooed [Fig. 4(a)].

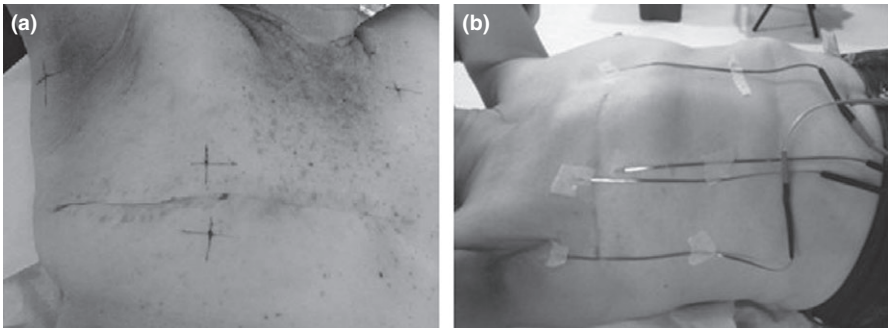

FIG. 4. Patient skin measurement points tattooed during the computed tomography scan (a). Skin MOSFETS positioning on the patient prior treatment (b).

A dose of 2 Gy per fraction for a total dose of 50 Gy was prescribed (PTV average dose) for all patients and both techniques according to the institutional protocol. Each plan was evaluated by analyzing PTV coverage and the dose-volume histograms. The 3DCRT technique was performed using two oblique opposing tangential fields (with field-in-field technique) with 4 MV energy. The VMAT technique was performed with 6 MV using two partial arcs. Bolus (1 cm) was used to increase the skin dose in the last 10 fractions of the 25 fractions in both techniques.

For each patient, the MOSFET detectors were positioned on the respective tattoos and properly secured with adhesive tape [Fig. 4(b)]. The normal sequence of treatment was carried out and the dose values were registered for each point at the end of the treatment. These were compared with the values of the predicted dose on the TPS. The TPS calculations were performed at the depth of about 1 mm under the skin.

The *in-vivo* measurements were performed for at least five fractions with bolus and five fractions without bolus, in order to increase the accuracy and reproducibility of the results. Each MOSFET was properly fixed on the initially referenced point on the patient skin for all measurements. After the end of the treatment, the MOSFET readings at each point were recorded. The measured dose for each position was then compared with the dose calculated by the TPS.

For each patient, the mean dose and the variability at each point were obtained. For a better interpretation of the results, the difference between the measured (D_M) and the calculated dose by the TPS (D_{TPS}) for each point was expressed as a percentage according to the Eq. (1):

$$\nabla\% = \frac{D_M - D_{TPS}}{D_{TPS}} \quad (1)$$

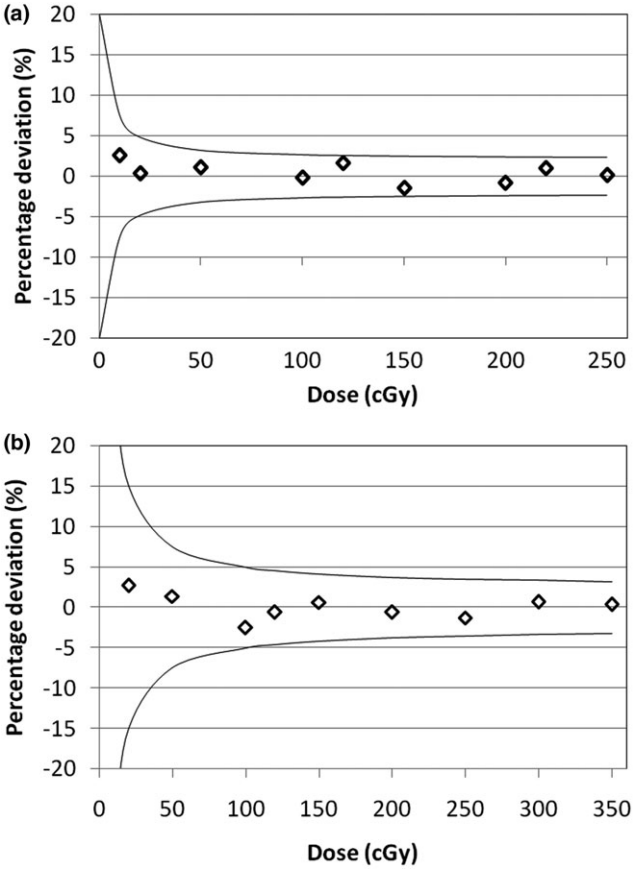

FIG. 5. Linearity behavior of MOSFET detector for 4 MV (a) and 6 MV (b) energy.

3 | RESULTS

3.A | MOSFET measurement system characterization

3.A.1 | Linearity and reproducibility

Figure 5 represents the MOSFET dose dependence for 4 MV (a) and 6 MV (b) beams. The results were adjusted by a linear function $a\,x + b$, where x = number of monitor units (MU) and a and b are adjustable variables. The percent deviation of the measurement results from the fitting function can be seen in the graphs of Fig. 5. The uncertainty lines correspond to the 2σ value (95.4% confidence interval) extracted from different measurements for the same MU. It was found that the MOSFET system has a reproducible response, and shows good linear dependence in the dose range analyzed for both energies.

3.A.2 | Angular dependence

The results are presented in the Fig. 6, for both studied energies. The standard deviations (%σ) obtained from all the considered

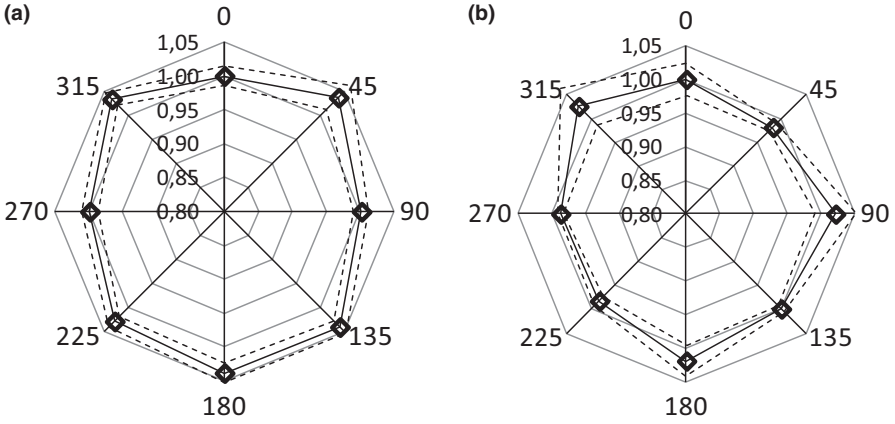

FIG. 6. MOSFET angular response for 4 MV (a) and 6 MV (b).

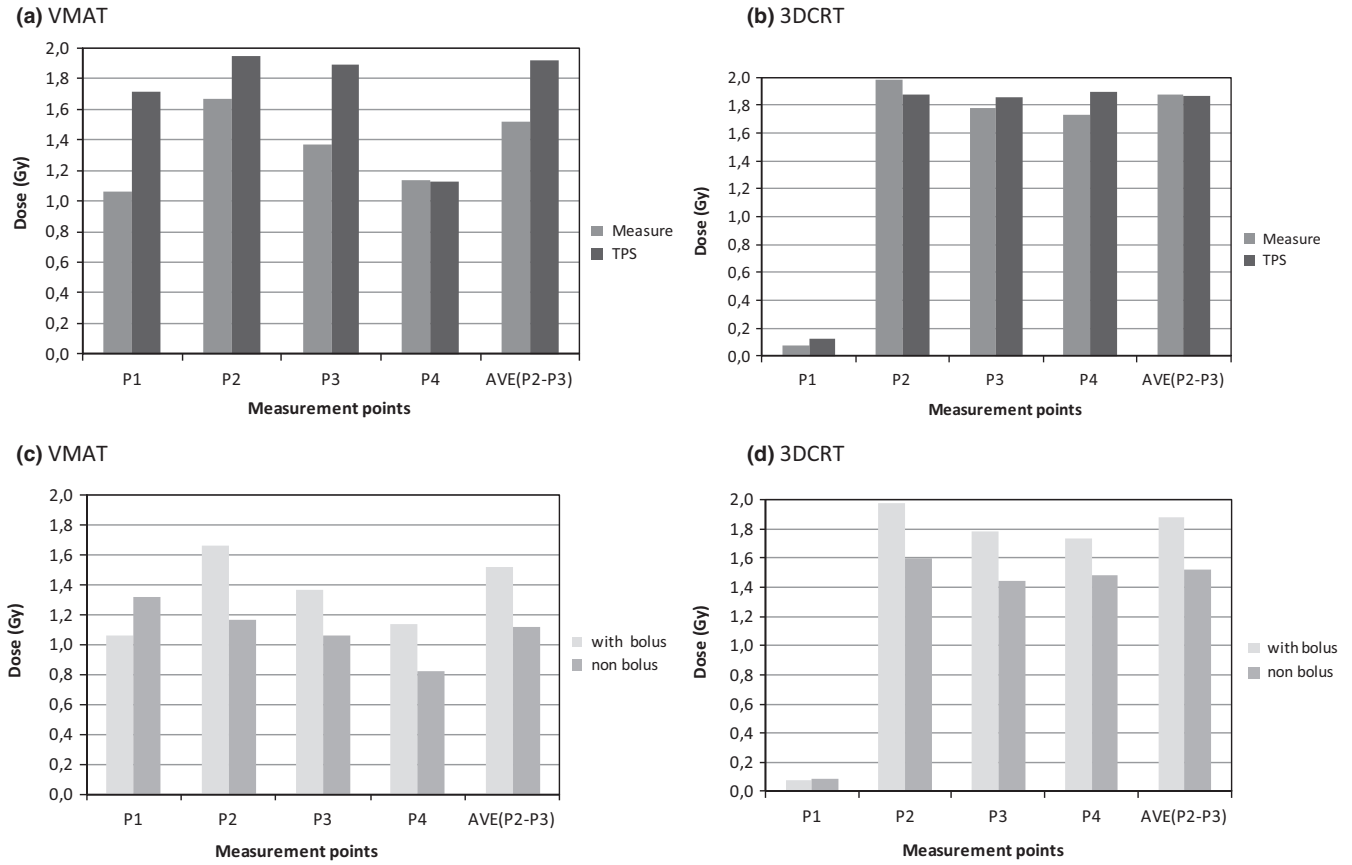

FIG. 7. Difference between the measured and expected (TPS) dose, with bolus, at each point in the anthropomorphic phantom for volumetric modulated arc therapy (VMAT) (a) and three dimensional conformal radiation therapy (3DCRT) (b). Comparison of the measured dose with and without bolus for VMAT (c) and 3DCRT (d) technique. The locations of points P1–P4 are described in Section 2.C and shown in Fig. 3.

directions were 1.86% and 1.67%, for 4 and 6 MV respectively, which are comparable within the ±2% variation over 360° as stated by the manufacturer.

3.B | Phantom dose measurement

The results of the 3DCRT and VMAT plan irradiation of the female anthropomorphic phantom (D_M) were compared with TPS calculated values (D_{TPS}) with and without bolus.

In Fig. 7 one can observe the difference between measured *vs.* calculated values as well as with *vs.* without bolus for both VMAT and 3DCRT.

As expected, partially due to the lower beam energy used, the measured surface dose presented higher values with 3DCRT (4 MV beam) technique compared with VMAT (6 MV beam) on the points above the PTV [Points P_2 and P_3 in Figs. 7(a) and 7(b)]. The anatomical upper inner quadrant of the contralateral breast (P_1) showed higher dose to the surface with VMAT technique but within the locally accepted tolerance limit (less or equal to 20 Gy in total). In Figs. 7(c) and 7(d), one observes the surface dose difference at the surface of the phantom with and without bolus.

3.C | Patient dose measurement

The obtained difference using the Eq. (1), ranged between 10% and 20% according to the considered points P_1–P_4 [Figs. 8(a) and 8(b)]. Analyzing the graphs in Figs. 8(c) and 8(d), the difference between the measured dose can be verified also "with bolus" vs "without bolus" for both 3DCRT and VMAT. In both cases, 80% of all measurements were within the range of ±20%, acceptance value for imprecision of the calculation of the dose by TPS recommended by the AAPM.[38]

4 | DISCUSSION

4.A | Phantom doses

In both VMAT and 3DCRT techniques, it is evident from Figs. 7(a) and 7(b) that, as expected, the surface dose with bolus is higher than to the surface dose without bolus. The obtained results agree with the literature, relating the increase of surface dose with the bolus presence on the irradiated area. The difference of measured and TPS calculated values are within the ±20%, corresponding to the

accepted value for the imprecision of dose calculation recommended by the AAPM (20% in the buildup region).[38]

4.B | Patient doses

In both VMAT and 3DCRT techniques, it is also evident from Figs. 8(a) and 8(b) that, as expected, the skin dose with bolus is superior to the skin dose without bolus. The obtained doses in all the points, except on P_1, are consistent with the expected results. This might be due to the fact that, for patients, several different plans were used and the observed measured values are an average of several different geometries. Additionally, the effect of bolus is more evident in the VMAT than in the 3DCRT.

Comparing the skin dose at different points, at P_1, anatomical upper inner quadrant of the contralateral breast, on average, the measured dose was lower than the dose calculated by the TPS for the 4 MV energy with the 3DCRT technique. This fact implies an overestimating of the dose in the P_1. However, for the VMAT technique (6 MV) the TPS underestimates the dose at this point with an average difference of 22.8% in patients. At P_2 and P_3 the average measured doses agree with TPS calculation (<4%). In general, P_4 is located in an area that presents large differences for both techniques (<10%).

Similar to the *in-phantom* experiments, no correction factors were applied to the *in-vivo* measurements. The same disparity trend between the measured and calculated values by the TPS was verified, compared to the results obtained in the phantom. Based on the analysis of the surface dose at the measurements points, it was verified that the points P_1 and P_4, corresponding to the anatomical upper inner quadrant of the contralateral breast and to the axillary area, present higher variability values, between calculated and measured, for the two treatment modalities, 3DCRT and VMAT. Since these points are located outside the area directly covered by the treatment fields, they are high dose gradient zones where the calculation is more imprecise. These are also subject to uncertainties of patient positioning and movement. In both techniques, the points on the PTV (P_2 and P_3), present higher homogeneity between calculated and measured doses. However, comparing the two treatment techniques, it was found that in the VMAT the TPS tends to underestimate the dose for these two points, contrary to the 3DCRT that tends to overestimate. These results are concordant in the two treatment phases with and without bolus. With the addition of the bolus in the final phase of treatment (after 15 treatment fractions without bolus), there was an increase of surface dose in the range of 5 to 20%, which is more significant in the VMAT technique. This variation from VMAT to 3DCRT can be compensated by changing

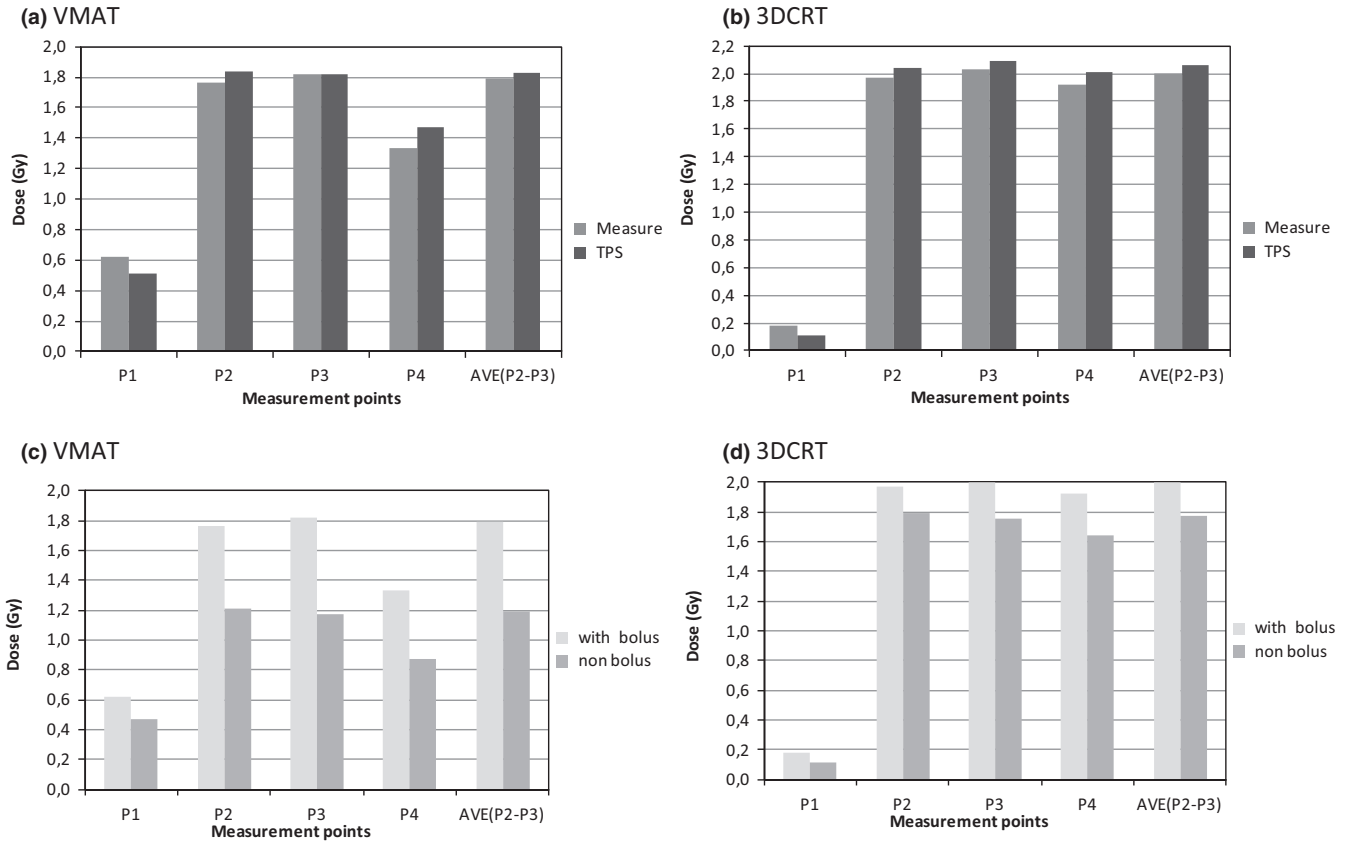

FIG. 8. Average measured and expected (treatment planning system) doses with bolus at each point in patients for volumetric modulated arc therapy (VMAT) (a) and three dimensional conformal radiation therapy (3DCRT) (b). Comparison of the measured dose with and without bolus for VMAT (c) and 3DCRT (d) technique.

the bolus thickness in the cases where an increase or a decrease of surface dose is desirable.

5 | CONCLUSIONS

From the measurements made in the female anthropomorphic phantom RANDO, considering the treatment plan performed in the TPS, and without any correction factors, there was some discrepancy between the measured and the calculated values by the TPS, with more evidence for plan without bolus. However, this difference was within the ±20% error range, the value referred in the AAPM-TG 53 for the TPS calculation imprecision in the buildup region. These measurements also demonstrate that the surface dose increased in the presence of the bolus when considering VMAT and 3DCRT. This increased surface dose is clearly higher in the VMAT technique. Since the treatment plan is very similar to that performed for treatment of patients with breast carcinoma, measurements using the RANDO phantom seem to indicate an easy and straightforward method of verifying surface dose (*in-vivo*) applicable in actual clinical situations. It should be noted that this method may be used in patients with other pathologies, always taking into account the associated error.

ACKNOWLEDGMENTS

The authors would like to acknowledge the radiotherapy technologists for their availability during *in-vivo* measurements throughout the treatment time.

CONFLICT OF INTEREST

No conflicts of interest.

REFERENCES

1. Herst PM. Protecting the radiation-damaged skin from friction: a mini review. *J Med Radiat Sci*. 2014;61:119–125.
2. Harris R, Beardmore C, Bolderston A, et al. Practice guidelines skin care advice for patients undergoing radical external beam megavoltage radiotherapy. *Radiother Oncol*. 2015;115:S919.
3. Dörr W. Skin and other reactions to radiotherapy – clinical presentation and radiobiology of skin reactions. *Radiat Ther Oncol Basel*. 2006;39:96–101.
4. von Essen F. Radiation tolerance of the skin. *Acta Radiol Ther Phys Biol*. 1969;8:311–330.
5. Pignol J-P, Olivotto I, Rakovitch E, et al. A multicenter randomized trial of breast intensity-modulated radiation therapy to reduce acute radiation dermatitis. *J Clin Oncol*. 2008;26:2085–2092.
6. Soleymanifard S, Aledavood SA, Noghreiyan AV, et al. In vivo skin dose measurement in breast conformal radiotherapy. *Contemp Oncol (Pozn)*. 2016;20:137–140.
7. Hsu S-H, Chen Y, Roberson P, et al. Assessment of skin dose for breast chest wall radiotherapy as a function of bolus material. *Phys Med Biol*. 2008;53:2593–2606.
8. Amber KT, Shiman MI, Badiavas EV, et al. The use of antioxidants in radiotherapy-induced skin toxicity. *Integr Cancer Ther*. 2014;13:38–45.
9. Andic F, Ors Y, Davutoglu R, et al. Evaluation of skin dose associated with different frequencies of bolus applications in post-mastectomy three-dimensional conformal radiotherapy. *J Exp Clin Cancer Res*. 2009;28:1–7.
10. Akino Y, Das IJ, Bartlett GK, Zhang H, Thompson E, Zook JE. Evaluation of superficial dosimetry between treatment planning system and measurements for several breast cancer treatment techniques. *Med Phys*. 2013;40:011714-1–011714-6.
11. Panettieri V, Barsoum P, Westermark M, Brualla L, Lax I. AAA and PBC calculation accuracy in the surface build-up region in tangential beam treatments. Phantom and breast case study with the Monte Carlo code PENELOPE. *Radiother Oncol*. 2009;93:94–101.
12. International Commission on Radiation Units and Measurement. *Determination of Dose Equivalents Resulting from External Radiation Sources*. ICRU Report 39, Washington DC: ICRU; 1985.
13. International Commission on Radiation Protection. *Recommendations of the International Commission on Radiological Protection*. ICRP Publication 26, Oxford, UK, Pergamon Press; 1977.
14. Kry SF, Smith SA, Weathers R, Stovall M. Skin dose during radiotherapy: a summary and general estimation technique. *J Appl Clin Med Phys*. 2012;13:20–34.
15. Chakarova R, Gustafsson M, Bäck A, et al. Superficial dose distribution in breast for tangential radiation treatment, Monte Carlo evaluation of eclipse algorithms in case of phantom and patient geometries. *Radiother Oncol*. 2012;102:102–107.
16. Kwan IS, Rosenfeld AB, Qi ZY, et al. Skin dosimetry with new MOSFET detectors. *Radiat Measur*. 2008;43:929–932.
17. Court LE, Tishler R, Xiang H, Allen AM, Makrigiorgos M, Chin L. Experimental evaluation of the accuracy of skin dose calculation for a commercial treatment planning system. *J Appl Clin Med Phys*. 2008;9:29–35.
18. Nakano M, Hill RF, Whitaker M, Kim JH, Kuncic Z. A study of surface dosimetry for breast cancer radiotherapy treatments using gafchromic EBT2 film. *J Appl Clin Med Phys*. 2012;13:83–97.
19. Quach KY, Morales J, Butson MJ, Rosenfeld AB, Metcalfe PE. Measurement of radiotherapy x-ray skin dose on a chest wall phantom. *Med Phys*. 2000;27:1676–1680.
20. Almberg SS, Lindmo T, Frengen J. Superficial doses in breast cancer radiotherapy using conventional and IMRT techniques: a film-based phantom study. *Radiother Oncol*. 2011;100:259–264.
21. Hurwitz LM, Yoshizumi TT, Reiman RE, et al. Radiation dose to the female breast from 16-MDCT body protocols. *AJR*. 2006;186:1718–1722.
22. Alnawaf H, Butson M, Yu PK. Measurement and effects of MOSKIN detectors on skin dose during high energy radiotherapy treatment. *Austr Phys Eng Sci Med*. 2012;35:321–328.
23. Jong WL, Wong JH, Ung NM, et al. Characterization of MOSkin detector for in vivo skin dose measurement during megavoltage radiotherapy. *J Appl Clin Med Phys*. 2014;15:120–132.
24. Cheung T, Butson MJ, Yu PK, et al. Energy dependence corrections to MOSFET dosimetric sensitivity. *Austr Phys Eng Sci Med*. 2009;32:16–20.
25. Gopiraj A, Ramasubramanian V. Entrance and exit dose measurements with MOSFET detectors during radiotherapy treatments. *Austral-Asian J Cancer*. 2009;8:151–158. ISSN-0972-2556.
26. Kinhikar RA, Murthy V, Goel V, et al. Skin dose measurements using MOSFET and TLD for head and neck patients treated with tomotherapy. *Appl Radiat Isot*. 2009;67:1683–1685.
27. Scalchi P, Francescon P. Calibration of a MOSFET detection system for 6-MV in vivo dosimetry. *Int J Radiat Oncol Biol Phys*. 1998;40:987–993.
28. Gopiraj A, Billimagga RS, Ramasubramanian V. Performance characteristics and commissioning of MOSFET as an in-vivo dosimeter for

high energy photon external beam radiation therapy. *Rep Pract Oncol Radiother*. 2008;13:114–125.
29. Kohno R, Hirano E, Nishio T, et al. Dosimetric evaluation of a MOSFET detector for clinical application in photon therapy. *Radiol Phys Technol*. 2008;1:55–61.
30. Kohno R, Hirano E, Kitou S, et al. Evaluation of the usefulness of a MOSFET detector in an antropomorphic phantom for 6MV photon beam. *Radiol Phys Technol*. 2010;3:104–112.
31. Soubra M, Cyger J, Mackay G. Evaluation of a dual bias dual metal oxide-silicon semicondutor field effect transistor detector as radiation dosimeter. *Med Phys*. 1994;21:567–572.
32. Ramani R, Russell S, O'Brien P. Clinical dosimetry using MOSFETs. *Int J Oncol Biol Phys*. 1997;37:959–964.
33. Vasile G, Vasile M, Duliu OG. In vivo dosimetry measurements for breast radiation treatments. *Rom Rep Phys*. 2012;64:728–736. www.rrp.infim.ro/2012_64_3/art08Vasile.pdf
34. Essers M, Mijnheer BJ. In vivo dosimetry during external photon beam radiotherapy. *Int J Radiat Oncol Biol Phys*. 1999;43:245–259.
35. Fischbach M, Hälg RA, Hartmann M, et al. Measurement of skin and target dose in post-mastectomy radiotherapy using 4 and 6 MV photons beams. *Radiat Oncol*. 2013;8:1–5.
36. Rijken J, Kairn T, Crowe S, Muñoz L, Trapp J. A simple method to account for skin dose enhancement during treatment planning of VMAT treatments of patients in contact with immobilization equipment. *J Appl Clin Med Phys*. 2018;19:239–245.
37. IAEA. Absorbed dose determination in external beam radiotherapy – an international code of practice for dosimetry based on standards of absorbed dose to water, TRS 398, Vienna; 2000.
38. American Association of Physicists in Medicine. Task Group 53: quality assurance for clinical radiotherapy treatment planning. *Med Phys*. 1998;25:1773–1829.